fractal and fractional

MDPI

Article

Quantization-Based Event-Triggered H_∞ Consensus for Discrete-Time Markov Jump Fractional-Order Multiagent Systems with DoS Attacks

Yi Lu [1], Xiru Wu [1,*], Yaonan Wang [2], Lihong Huang [3] and Qingjin Wei [4]

[1] School of Electronic Engineering and Automation, Guilin University of Electronic Technology, Guilin 541004, China; ylu_1027@163.com
[2] College of Electrical and Information Engineering, Hunan University, Changsha 410114, China; yaonan@hnu.edu.cn
[3] Department of Mathematics and Computer Science, Changsha University, Changsha 410022, China; lhhuang@hnu.edu.cn
[4] College of Artificial Intelligence and Manufacturing, Hechi University, Hechi 547000, China
* Correspondence: xiruwu@guet.edu.cn

Abstract: This paper investigates the H_∞ consensus problem of discrete-time Markov jump fractional-order multiagent systems (DTMJFOMASs) under denial-of-service (DoS) attacks. By applying the short-memory principle, we can obtain discrete-time Markov jump multiagent systems with partially unknown probabilities. A novel quantized event-triggering mechanism (QETM), based on a mode-dependent logarithmic quantizer, is proposed to enhance transmission efficiency among multiagents. A distributed controller with quantized output is developed. Sufficient conditions are provided to ensure the system achieves H_∞ consensus through Lyapunov stability theory. Finally, two examples are given to verify the effectiveness of the proposed model.

Keywords: quantized event-triggering mechanism; Markov jump fractional-order multiagent systems; H_∞ consensus; denial-of-service attacks

Citation: Lu, Y.; Wu, X.; Wang, Y.; Huang, L.; Wei, Q. Quantization-Based Event-Triggered H_∞ Consensus for Discrete-Time Markov Jump Fractional-Order Multiagent Systems with DoS Attacks. *Fractal Fract.* **2024**, *8*, 147. https://doi.org/10.3390/fractalfract8030147

Academic Editor: Inés Tejado

Received: 24 January 2024
Revised: 22 February 2024
Accepted: 28 February 2024
Published: 2 March 2024

1. Introduction

Multiagent systems (MASs) have been extensively utilized in multi-robot formation control [1], multiple single-link robotic arm systems (SLRASs) [2], and smart grids [3]. The consensus or synchronization problem has always been a central issue in MASs, aiming to achieve agreement among multiagents through communication. The issue of consensus in MASs has been extensively explored, including H_∞ consensus [4,5], event-triggered consensus [6–8], distributed consensus [9], finite/fixed-time consensus [10,11], and so on.

It is worth mentioning that the research on MASs assumes that system parameters and structures are deterministic. However, in practical systems, system parameters and structures may change because of unexpected factors (external disturbances, hardware failures, etc.) [12,13]. To resolve the above situation, the Markov jump process is introduced into MASs, realizing uncertain jumps through stochastic transition probabilities. This has been studied by many scholars in various ways [14–20]. The finite-time leader-following consensus issue in MASs with Markov switching parameters has been studied in [14]. Additionally, the problem of leader-following consensus in semi-Markov jump multiagent systems was examined in [15]. In [16,17], the authors addressed the event-triggered consensus problem for Markov jump multiagent systems (MJMASs). Considering quantized multi-channel transmission, Huo et al. [18] explored the output feedback consensus control strategy to examine the H_∞ consensus problem in MJMASs. The synchronization problem of heterogeneous MJMASs was studied in [19] using a collaborative output quadratic controller. In [19,20], the H_∞ consensus issue of the MJMASs was discussed with incomplete transition probabilities. Given the analysis above, MJMASs with partially unknown

transition probabilities have not been extensively studied. Thus, this drives the research in this paper.

Furthermore, we explore fractional-order multiagent systems (FOMASs). FOMASs are considered to be more reliable, flexible, and accurate in modeling the systems than integer-order MASs. Fractional-order systems are widely used for dynamical systems with memory or hereditary features [21–23]. The paper addresses the consensus challenges in FOMASs (DTFOMASs). The containment control problem for DTFOMASs with time delays was discussed in [24]. Ref. [23] focused on the H_∞ consensus problem of DTFOMASs with finite-dimensional memory states. According to review [25], we consider a class of systems that combines MJMASs and FOMASs, referred to as DTMJFOMASs.

High-frequency communication among multiagents leads to severe congestion in limited channels. Signal quantization is a prevalent control strategy in digital communication for optimizing network communication resources. In practical applications, the event-triggering mechanisms (ETMs) [6–8,11,26–29] are instrumental in lowering communication burdens among multiagents and conserving network resources. Building upon this, MAS consensus has been studied by combining quantization strategies and ETMs. The application of an event-triggered pinning control was discussed in [30] to solve the containment consensus problem in MASs with quantized communication. Under the framework of quantized event-triggered control, Zhang et al. [31] examined the secure consensus problem for linear MASs. In [32], a data-driven event-triggered control algorithm was introduced for nonlinear MASs utilizing uniform quantization in the encoding–decoding scheme. By integrating ETM and a quantized control technique, Ref. [33] addressed the distributed adaptive optimization problem of nonstrict feedback FOMASs with uncertainty. However, the general quantizers [30–35] are typically determined by fixed threshold parameters. This contributes to the decline in system performance. Hence, resembling Markov modes, a quantization strategy with dynamic switching is investigated in this study.

The consensus issue in open MASs poses a threat that cannot be ignored. Denial-of-service (DoS) attacks manifest as network assaults that deplete bandwidth, overload servers, or deplete system resources [36]. Thus, how to enhance the robustness of system control is a challenging issue. Ref. [27] investigated DoS attacks governed by a Markov process and explored a model predictive control approach to enhance system robustness. To address network systems with DoS attacks, an event-triggered cognitive controller was introduced in [37]. In [38], a mode-dependent H_∞ consensus approach was developed to tackle the leader-following consensus problem affected by DoS attacks. In general, there are two types of stochastic processes for random DoS attacks: the Markov jump process [27,37] and the Bernoulli distribution process [38]. Until now, the impact of DoS attacks with a Bernoulli distribution process on DTMJMASs has not been adequately investigated. This motivates us to undertake further research.

Building upon the aforementioned discussions, this paper investigates the H_∞ consensus problem of DTMJFOMASs with distributed controllers. A mode-dependent QETM is introduced to mitigate communication overhead. The contributions of this paper are articulated as follows:

1. Compared to MJMASs and FOMASs, we address the more generalized H_∞ consensus problem for DTMJFOMASs, which takes into account incomplete probabilistic Markov processes and external disturbances.
2. A mode-dependent distributed controller with quantized inputs is developed, and DoS attacks obeying a Bernoulli distribution are addressed to enhance the robustness of the system.
3. Considering the high-frequency communication between MASs, a mode-dependent approach to quantization is introduced. Compared with the traditional triggering strategy, the QETM has both a lower triggering frequency and meets the system performance requirements.

The remaining structure of the paper is outlined as follows: In Section 2, some foundational knowledge is provided. Section 3 introduces DTMJFOMASs and designs QETM. H_∞

performance is analyzed in Section 4. Section 5 validates the effectiveness of the proposed model. Lastly, Section 6 summarizes this paper.

Notations: Some symbols in this article are as follows: $\mathbb{Z}^+$ represents a positive real number. I is an identity matrix. $\mathbb{R}^n$ denotes an n-dimensional vector. Pr and acot represent the Prob and arccot function, respectively. $\|\cdot\|$ and $\otimes$ represent the two norm and the multiplication cross, respectively. Finally, 1_n is an n-dimensional vector with all ones in it, i.e., $[1, \ldots, 1]^T \in \mathbb{R}^n$.

2. Preliminaries

Definition 1 ([39]). *The Grünwald–Letnikov fractional derivative of $f(t)$ is outlined in*

$$ {}_a^G D_t^\alpha f(t) = \lim_{h\to 0} h^{-\alpha} \sum_{\varpi=0}^{\left[\frac{t-a}{h}\right]} (-1)^\varpi \begin{bmatrix} \alpha \\ \varpi \end{bmatrix} f(t-\varpi h), \tag{1} $$

where $\alpha \in \mathbb{Z}^+$, h is the sampling interval.

$$ \begin{bmatrix} \alpha \\ \varpi \end{bmatrix} = \begin{cases} 1 & \varpi = 0, \\ \frac{\alpha(\alpha-1)\cdots(\alpha-\varpi+1)}{\varpi!} & \varpi = 1,2,3,\cdots. \end{cases} $$

Let $c_\varpi(\alpha) = (-1)^\varpi \begin{bmatrix} \alpha \\ \varpi \end{bmatrix}$. Obviously, $|c_\varpi(\alpha)| \le \frac{\alpha^j}{\varpi!}$, $c_\varpi(\alpha)$ is the absolutely summable sequence.

Based on the works in [23], the discrete-time bounded form of (1) can be expressed as

$$ D_t^\alpha f(t) \approx \Delta_h^\alpha f(kh) = h^{-\alpha} \sum_{\varpi=0}^{k} c_\varpi(\alpha) f((k-\varpi)h). \tag{2} $$

Lemma 1 ([40]). *Given appropriately dimensioned matrices S_{11}, S_{12}, and S_{22}, the following matrix inequality is satisfied:*

$$ \begin{bmatrix} S_{11} & S_{12} \\ S_{12}^T & S_{22} \end{bmatrix} < 0 $$

if and only if

$$ S_{11} < 0,\ S_{22} - S_{12}^T S_{11}^{-1} S_{12} < 0, $$
$$ S_{22} < 0,\ S_{11} - S_{12} S_{22}^{-1} S_{12}^T < 0. $$

Lemma 2 ([41]). *Assuming appropriately dimensioned matrices X, Y, and diagonal matrix M exist with $MM \le I$, the following condition holds for any $\varepsilon > 0$:*

$$ XMY + (XMY)^T \le \varepsilon XX^T + \varepsilon^{-1} Y^T Y. $$

Lemma 3 ([16]). *If there be real matrices A, B, M, and N such that the following conditions hold for any $\epsilon > 0$:*

$$ \begin{bmatrix} M & A + \epsilon B^T \\ * & -\epsilon(N + N^T) \end{bmatrix} < 0, $$

then we have

$$ M + AN^{-1}B + B^T X^{-T} A^T < 0. $$

3. Materials and Methods

3.1. Problem Formulation

Consider a class of DTMJFOMASs with n identical agents:

$$\begin{cases} \Delta^{\alpha} x_i(k+1) = A_{\phi(k)} x_i(k) + B_{\phi(k)} u_i(k) + D_{\phi(k)} \omega_i(k) \\ y_i(k) = C_{\phi(k)} x_i(k) \\ z_i(k) = E_{\phi(k)} (x_i(k) - \frac{1}{n} \sum_{j=1}^{n} x_j(k)) \end{cases}, \tag{3}$$

where $x_i(k) \in \mathbb{R}^{n_x}$ is the state of the ith agent; $y_i(k) \in \mathbb{R}^{n_y}$ and $z_i(k) \in \mathbb{R}^{n_z}$ are the measured output and controlled output, respectively, of the ith agent; $\omega_i(k) \in \mathbb{R}^{n_\omega}$ is the disturbance input of the ith agent; and $u_i(k) \in \mathbb{R}^{n_u}$ is the control input of the ith agent. The matrices A, $B_{\phi(k)}$, $C_{\phi(k)}$, $D_{\phi(k)}$, $E_{\phi(k)}$ are the known real matrices. $\phi \in \mathcal{M} = \{1, \cdots, \mathfrak{m}\}$ is a Markov chain with the transition probability matrix (TPM) $\Pi = \{\pi_{\varsigma p}\}$:

$$\pi_{\varsigma p} = \Pr\{\phi(k+1) = p | \phi(k) = \varsigma\},$$

where $\sum_{p=1}^{\mathfrak{m}} \pi_{\varsigma p} = 1$ and $\pi_{\varsigma p} \in [0,\ 1]$. Within the TPM, there exist unspecified elements, illustrated by the 3rd-order matrix Π:

$$\Pi = \begin{bmatrix} \pi_{11} & * & * \\ * & \pi_{22} & * \\ * & * & \pi_{33} \end{bmatrix},$$

where "$*$" indicates an unknown element.

According to (2), the state variable can be articulated as

$$\Delta_{k+1}^{\alpha_i} x_i(k+1) = h^{-\alpha} \sum_{\varpi=0}^{k+1} c_{\varpi}(\alpha_i) x_i(k+1-\varpi) \tag{4}$$

Hence, $x_i(k+1)$ can be reformulated as

$$x_i(k+1) = (h^{\alpha} A + \alpha I_n) x_i(k) + h^{\alpha} B_{\phi(k)} u_i(k) + h^{\alpha} D_{\phi(k)} \omega_i(k) + \sum_{v=1}^{L} c_v(\alpha) x(k-v). \tag{5}$$

Let $\phi(k) = \varsigma$ and $x_i(k) = \left[x_i^T(k),\ x_i^T(k-1),\ \cdots,\ x_i^T(k-L)\right]^T$, then Equation (3) can be extended to

$$\begin{cases} x_i(k+1) = \mathcal{A}_{\varsigma} x_i(k) + \mathcal{B}_{\varsigma} u_i(k) + \mathcal{D}_{\varsigma} \omega_i(k) \\ y_i(k) = \mathcal{C}_{\varsigma} x_i(k) \\ z_i(k) = \mathcal{E}_{\varsigma} (x_i(k) - \frac{1}{n} \sum_{j=1}^{n} x_j(k)) \end{cases}, \tag{6}$$

where

$$\mathcal{A}_{\varsigma} = \begin{bmatrix} h^{\alpha} A_{\varsigma} + \alpha I_n & c_1 I_n & \cdots & c_L I_n \\ I_n & 0 & \cdots & 0 \\ 0 & I_n & \cdots & 0 \\ \vdots & \vdots & \ddots & \vdots \\ 0 & 0 & \cdots & 0 \end{bmatrix}, \mathcal{B}_{\varsigma} = \begin{bmatrix} h^{\alpha} B_{\varsigma} \\ 0 \\ \vdots \\ 0 \end{bmatrix},$$

$$\mathcal{C}_{\varsigma}^T = \begin{bmatrix} C_{\varsigma} \\ 0 \\ \vdots \\ 0 \end{bmatrix}, \mathcal{D}_{\varsigma} = \begin{bmatrix} h^{\alpha} D_{\varsigma} \\ 0 \\ \vdots \\ 0 \end{bmatrix}, \mathcal{E}_{\varsigma}^T = \begin{bmatrix} E_{\varsigma} \\ 0 \\ \vdots \\ 0 \end{bmatrix}.$$

Assumption 1. *The pair $(\mathcal{A}, \mathcal{B})$ is stabilizable.*

Assumption 2. *The pair $(\mathcal{A}, \mathcal{C})$ is observable.*

Remark 1. *According to Theorem 8.19 in [42], it is evident that if $h^{\alpha}A_{\varsigma}+\alpha \leq 1$, then DTMJ-FOMASs (6) is stabilizable. That is, Assumption 1 is equivalent to the condition $h^{\alpha}A_{\varsigma}+\alpha \leq 1$. As per [43], it is known that (A, C) being observable in (3) is equivalent to Assumption 2.*

3.2. Quantized Event-Triggered Mechanism

A mode-dependent logarithmic quantizer can be outlined in

$$q^{i}_{\psi(k)}(v^{i})=\begin{cases} v^{ij}_{\psi(k)}, & \frac{v^{ij}_{\psi(k)}}{1+\delta^{i}_{\psi(k)}} \leq v^{i} \leq \frac{v^{ij}_{\psi(k)}}{1-\delta^{i}_{\psi(k)}} \\ 0, & v^{i}=0 \\ -q^{i}_{\psi(k)}(-v^{i}), & v^{i}<0 \end{cases}, \tag{7}$$

where $\delta_{\psi(k)}=[(1-\rho_{\psi(k)})/(1+\rho_{\psi(k)})], 0<\delta_{\psi(k)}<1, 0<\rho_{\psi(k)}<1$. $\psi \in \mathcal{N}=\{1, \cdots, \mathfrak{N}\}$ is a Markov chain with the TPM $\Theta=\{\theta_{\varrho q}\}$:

$$\theta_{\varrho q}=\Pr\{\psi(k+1)=q|\psi(k)=\varrho\},$$

where $\sum_{q=1}^{\mathfrak{n}}\theta_{\varrho q}=1$ and $\theta_{\varrho q} \in [0,\ 1]$.

Let $\psi(k)=\varrho$. $Q(v)=[q^{1}_{\varrho}(v_1), \cdots, q^{s}_{\varrho}(v_s)]^{T}$ be defined as the set of logarithmic quantization levels. As per [44], $q^{i}_{\varrho}(v^{i})$ is a sector with bounds; then there is

$$Q_{\varrho}(y(k))=(1+\mathcal{H}_{\varrho}(k))y(k),$$

where $\mathcal{H}_{\varrho}=[\mathcal{H}^{1}_{\varrho}(k), \cdots, \mathcal{H}^{i}_{\varrho}(k)]^{T}$ and $|\mathcal{H}^{i}_{\varrho}(k)| \leq \delta^{i}_{\varrho}<1$.

To mitigate communication overhead, this study examines the logarithmic quantizer into the ETM, called QETM. For each agent, the trigger instant by the following condition:

$$k^{i}_{d+1}=\min_{k\in\mathbb{N}}\{k>k^{i}_{d} \mid \sigma(k)\eta^{\mathrm{T}}_{i}(k)\Omega_1\eta_i(k)-e^{\mathrm{T}}_{i}(k)\Omega_2 e_i(k) \leq 0\}, \tag{8}$$

where $\sigma(k)=\varrho_1+(\varrho_2-\varrho_1)\frac{2}{\pi}\mathrm{acot}(\varepsilon_0\|\mathfrak{y}(k)\|^{2})$ $(0<\varrho_1<\varrho_2<1,\ \varepsilon_0>0)$ is a threshold parameter, k^{i}_{d} denotes the last trigger instant of agent i, Ω_1 and Ω_2 represent the weighting matrices. $\eta(k)=Q(y(k))$, and the measurement error is determined as follows

$$e(k)=\eta(k)-\eta(k^{i}_{d})$$

Remark 2. *A mode-dependent QETM is introduced in this paper, demonstrating enhanced generalization compared to traditional triggering mechanisms.*

1. *A quantizer with dynamic switching features is more able to emphasize the robustness of the system, while traditional quantizers [30–34] lack the capability to achieve system stability through dynamic adjustments.*
2. *If the quantizer $q^{i}_{\psi(k)}(v^{i})=v^{i}$, then the QETM can degenerate into the dynamic event-triggered mechanism [7,11,26].*
3. *If the quantizer $q^{i}_{\psi(k)}(v^{i})=v^{i}$ and $\sigma(k)$ is a constant, then the QETM can transform into the static event-triggered mechanism [6,27,28].*

Remark 3. *In the QETM (8), the adaptive parameter $\sigma(k)$ is taken into consideration. It is apparent that the dynamic parameter $\sigma(k)$ changes in real time based on the quantized error $\eta(k)$.*

3.3. Mode-Dependent Distributed Control Protocol

DoS attacks lead to network communication disruptions, which result in packet loss and affect system stability. Under DoS attacks, the distributed control protocol with quantization is considered as follows:

$$u_i(k) = \begin{cases} c\beta(k)K_{\phi(k)}\sum_{j=1}^{N} g_{ij}(\eta_j(k) - \eta_i(k)), & i \neq j \\ 0, & i = j \end{cases}, \tag{9}$$

where $c > 0$ is a scalar, $K_{\phi(k)}$ is a gain matrix, and $\beta(k) \in [0,\ 1]$ conforms to a Bernoulli distribution, representing stochastic packet loss. If it equals 1, it signifies successful data transmission to the agents; otherwise, it indicates data loss.

$$\begin{cases} \Pr\{\beta(k) = 1\} = \mathbb{E}\{\beta(k)\} = \bar{\beta} \\ \Pr\{\beta(k) = 0\} = 1 - \mathbb{E}\{\beta(k)\} = 1 - \bar{\beta}. \end{cases}$$

Remark 4. *The considered network framework primarily illustrates the control process of the ith agent, while the other agents operate similarly to the ith agent, as depicted in Figure 1. The framework mainly consists of the ith agent, a sensor, an event trigger, a controller, a zero-order holder (ZOH), and an actuator. Utilizing a topological structure, the ith agent interacts with other agents, forming a communication network. Given the impact of a DoS attack, the consensus problem of DTMJFOMASs is addressed.*

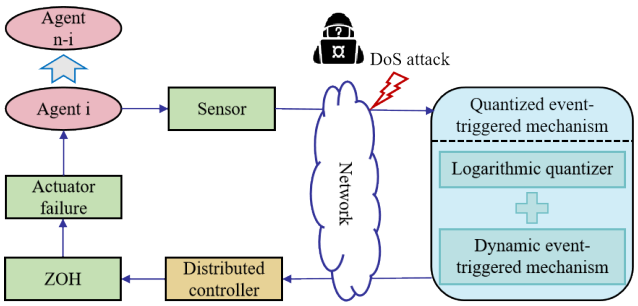

Figure 1. The framework of the DTMJFOMASs with QETM.

3.4. Model Transformation

Upon substituting control protocol (9) into DTMJFOMASs (6), one obtains

$$\begin{cases} x(k+1) = (I_n \otimes \mathcal{A}_\varsigma)x(k) + c\bar{\beta}(\mathcal{L} \otimes \mathcal{B}_\varsigma K_\varsigma(I_n + \mathcal{H}_\varrho)\mathcal{C}_\varsigma)x(k) \\ \qquad\qquad -c(\beta(k) - \bar{\beta})(\mathcal{L} \otimes \mathcal{B}_\varsigma K_\varsigma)e(k) + (I_n \otimes \mathcal{D}_\varsigma)\omega(k) \\ z(k) = (\beth \otimes \mathcal{E}_\varsigma)x(k) \end{cases}, \tag{10}$$

where $x(k) = \mathrm{col}(x_i^T(k))$, $y(k) = \mathrm{col}(y_i^T(k))$, $z(k) = \mathrm{col}(z_i^T(k))$, $\omega(k) = \mathrm{col}(\omega_i^T(k))$, $\beth = I_n - \frac{1}{n}1_n 1_n^T$.

Let $\tilde{x}(k) = (\beth \otimes I_n)x(k)$. Based on $\beth\beth = \beth$ and $\beth\mathcal{L} = \mathcal{L}\beth$, the system (10) can be reformulated as

$$\begin{cases} \tilde{x}(k+1) = (I_n \otimes \mathcal{A}_\varsigma)\tilde{x}(k) + c\bar{\beta}(\mathcal{L} \otimes \mathcal{B}_\varsigma K_\varsigma(I_n + \mathcal{H}_\varrho)\mathcal{C}_\varsigma)\tilde{x}(k) \\ \qquad\qquad -c(\beta(k) - \bar{\beta})(\mathcal{L} \otimes \mathcal{B}_\varsigma K_\varsigma)e(k) + (I_n \otimes \mathcal{D}_\varsigma)\omega(k) \\ \tilde{z}(k) = (\beth \otimes \mathcal{E}_\varsigma)\tilde{x}(k) \end{cases} \tag{11}$$

For a given orthogonal matrix $\mathcal{Q} = [\mathcal{Q}_1, \mathcal{Q}_2]$ with $\mathcal{Q}_2 = 1/\sqrt{n}1_n$, such that $\mathcal{Q}^T \beth \mathcal{Q} = \text{diag}\{I_{n-1}, 0\}$ and $\mathcal{Q}^T \mathcal{L} \mathcal{Q} = \text{diag}\{\gamma_1, \cdots, \gamma_{n-1}, 0\}$. Then, one has

$$\begin{cases} \overline{x}_\iota(k+1) = (I_{n-1} \otimes \mathcal{A}_\varsigma + c\bar{\beta}\Gamma_1)\overline{x}_\iota(k) - c(\beta(k) - \bar{\beta})\Gamma_2 \overline{e}_\iota(k) + (I_{n-1} \otimes \mathcal{D}_\varsigma)\overline{\omega}_\iota(k) \\ \overline{z}_\iota(k) = (I_{n-1} \otimes \mathcal{E}_\varsigma)\overline{x}_\iota(k) \end{cases} \tag{12}$$

and

$$\begin{cases} \overline{x}_n(k+1) = \mathcal{A}_\varsigma \overline{x}_n(k) + \mathcal{D}_\varsigma \overline{\omega}_n(k) \\ \overline{z}_n(k) = 0 \end{cases}, \tag{13}$$

where
$\overline{x}(k) = [\overline{x}_\iota^T(k), \overline{x}_n^T(k)]^T$, $\overline{z}(k) = [\overline{z}_\iota^T(k), \overline{z}_n^T(k)]^T$,
$\overline{e}(k) = [\overline{e}_\iota^T(k), \overline{e}_n^T(k)]^T$, $\overline{\omega}(k) = [\overline{\omega}_\iota^T(k), \overline{\omega}_n^T(k)]^T$,
$\overline{x}_\iota(k) = [\overline{x}_1^T(k), \cdots, \overline{x}_{n-1}^T(k)]^T$, $\overline{e}_\iota(k) = [\overline{e}_1^T(k), \cdots, \overline{e}_{n-1}^T(k)]^T$,
$\overline{\omega}_\iota(k) = [\overline{\omega}_1^T(k), \cdots, \overline{\omega}_{n-1}^T(k)]^T$, $\overline{z}_\iota(k) = [\overline{z}_1^T(k), \cdots, \overline{z}_{n-1}^T(k)]^T$,
$\Gamma_1 = \text{diag}\{\gamma_1, \ldots, \gamma_{n-1}\} \otimes \mathcal{B}_\varsigma K_\varsigma (I_{n-1} + \mathcal{H}_\varrho)\mathcal{C}_\varsigma$,
$\Gamma_2 = \text{diag}\{\gamma_1, \ldots, \gamma_{n-1}\} \otimes \mathcal{B}_\varsigma K_\varsigma$.

It is evident that with $\overline{z}_\iota(k)$ being equivalent to $\overline{z}_i(k)$, the stability of DTMJFOMASs (3) implies the consensus attainment of subsystem (14).

$$\begin{cases} \hat{x}_\varkappa(k+1) = (\mathcal{A}_\varsigma + c\bar{\beta}\gamma_\varkappa \mathcal{B}_\varsigma K_\varsigma (I + \mathcal{H}_\varrho)\mathcal{C}_\varsigma)\hat{x}_\varkappa(k) \\ \qquad\qquad -\gamma_\varkappa \mathcal{B}_\varsigma K_\varsigma \hat{e}_\varkappa(k) + \mathcal{D}_\varsigma \hat{\omega}_\varkappa(k) \\ \hat{z}_\varkappa(k) = \mathcal{E}_\varsigma \hat{x}_\varkappa(k) \end{cases}, \tag{14}$$

where $\varkappa \in \{1, \cdots, n-1\}$.

Definition 2 ([45]). *The DTMJFOMASs (14) with $\hat{\omega}_\varkappa(k) = 0, \forall \varkappa \in \{1, \cdots, n-1\}$ are said to be mean-square asymptotic stability if it satisfies:*

$$\lim_{k\to\infty} \mathbb{E}\{\|e_i(k) - e_j(k)\|\}^2 = 0, \ \forall i, j \in \{1, \ldots, n-1\}. \tag{15}$$

Definition 3 ([46]). *Considering DTMJFOMASs (14) under DoS attacks and the H_∞ consensus performance metrics $\mu > 0$ based on distributed control protocols, stochastic stability can be attained if the following conditions are met:*

1. *If $\hat{\omega}(k) \equiv 0$, the system consensus is mean-square asymptotic stability, i.e., Definition (2) is met.*
2. *Under zero initial conditions, the following inequality holds for any non-zero $\hat{\omega}(k) \in L_2[0, \infty)$:*

$$\sum_{k=0}^{\infty} \mathbb{E}\{\hat{z}_\varkappa^T(k)\hat{z}_\varkappa(k)\} < \mu^2 \sum_{k=0}^{\infty} \mathbb{E}\{\hat{\omega}_\varkappa^T(k)\hat{\omega}_\varkappa(k)\}. \tag{16}$$

4. Main Results

In this section, firstly, the stochastic stability conditions for all agents are analyzed. Subsequently, the mean-square asymptotic stability and H_∞ performance conditions for the system (14) are established. Lastly, the design procedure for the distributed controller (9) with mode-dependent is showcased.

Theorem 1. *Under Assumptions 1 and 2, the DTMJFOMASs (14) with $\hat{\omega}_\varkappa(k) = 0$ exhibits stochastic consensus stability. Then, for any scalar $0 \le \varkappa \le n-1$, the following condition holds:*

$$\Lambda_\varkappa^{\varsigma\varrho} = \begin{bmatrix} \Lambda_{11} & 0 & \Lambda_{13} \\ * & -I & \Lambda_{23} \\ * & * & \Lambda_{33} \end{bmatrix} < 0,$$

where
$\mathcal{P}_{\varsigma\varrho} = \sum_{p=\mathcal{M}} \sum_{q=\mathcal{N}} \pi_{\varsigma p}\theta_{\varrho q} P_{pq}$,
$\Lambda_{11} = \mathcal{C}_\varsigma^T \mathcal{C}_\varsigma - P_{\varsigma\varrho}$, $\Lambda_{13} = (\mathcal{A}_\varsigma + \gamma_\varkappa \mathcal{B}_\varsigma K_\varsigma (I + \mathcal{H}_\varrho)\mathcal{C}_\varsigma)^T$,
$\Lambda_{23} = (\gamma_\varkappa \mathcal{B}_\varsigma K_\varsigma)^T$, $\Lambda_{33} = \mathcal{P}_{\varsigma\varrho}^{-1}$.

Proof. To analyze the stochastic consensus stability for the DTMJFOMASs (14) with $\hat{\omega}_\varkappa(k) = 0$, one considers the following Lyapunov function as

$$V_\varkappa(k, \phi(k), \psi(k)) = \hat{x}_\varkappa^T(k) P_{\phi(k),\psi(k)} \hat{x}_\varkappa(k),$$

and its expectation manifests as

$$\mathbb{E}\{\triangle V_\varkappa(k, \phi(k), \psi(k))\} = \mathbb{E}\{V_\varkappa(k+1, \phi(k+1), \psi(k+1)) - V_\varkappa(k, \phi(k), \psi(k))\}. \tag{17}$$

According to TPMs Π and Θ, we can obtain

$$\begin{aligned}
&\Pr\{\phi(k+1) = p, \psi(k+1) = q | \phi(k) = \varsigma, \psi(k) = \varrho\} \\
=&\Pr\{\phi(k+1) = p | \phi(k) = \varsigma, \psi(k) = \varrho\} \times \Pr\{\psi(k+1) = q | \phi(k) = \varsigma, \psi(k) = \varrho\} \\
=&\pi_{\varsigma p}\theta_{\varrho q}.
\end{aligned}$$

Thus, Equation (17) can be reduced to

$$\begin{aligned}
&\mathbb{E}\{\triangle V_\varkappa(k, \varsigma, \varrho)\} \\
\leq&\mathbb{E}\{\hat{x}_\varkappa^T(k+1)\mathcal{P}_{\varsigma\varrho}\hat{x}_\varkappa(k) - \hat{x}_\varkappa^T(k)P_{\varsigma,\varrho}\hat{x}_\varkappa(k) + \hat{x}_\varkappa^T(k)\mathcal{C}_\varsigma^T\mathcal{C}_\varsigma\hat{x}_\varkappa(k) - \hat{e}_\varkappa^T(k)\hat{e}_\varkappa(k)\} \\
=&\xi_\varkappa^T(k)\Lambda_\varkappa^{\varsigma\varrho}\xi_\varkappa(k),
\end{aligned} \tag{18}$$

where $\xi_\varkappa^T(k) = [\hat{x}_\varkappa^T(k),\ \hat{e}_\varkappa^T(k)]^T$.

Remark 5. *During the solution of Equation (18), a strategic use of an additional term* ($g(x) = \hat{x}_\varkappa^T(k)\mathcal{C}_\varsigma^T\mathcal{C}_\varsigma\hat{x}_\varkappa(k) - \hat{e}_\varkappa^T(k)\hat{e}_\varkappa(k)$) *was incorporated to simplify the solving process. Clearly,* $g(x) \geq 0$, *and the equation is valid.*

Using Lemma 1, it is easy to obtain $\Lambda_\varkappa^{\varsigma\varrho} < 0$. One can obtain

$$\mathbb{E}\{\triangle V_\varkappa(k, \varsigma, \varrho)\} \leq -\hbar\mathbb{E}\{\|\xi_\varkappa(k)\|^2\}, \tag{19}$$

where $\hbar = \min_{\varsigma=\mathcal{M},\ \varrho=\mathcal{N}}\{\lambda(\Lambda_\varkappa^{\varsigma\varrho})\}$ ($\hbar > 0$). Furthermore, we have

$$\mathbb{E}\{V_\varkappa(n+1, \varsigma, \varrho) - V_\varkappa(0, \varsigma, \varrho)\} \leq -\hbar\sum_{k=0}^{n}\mathbb{E}\{\|\xi_\varkappa(k)\|^2\}. \tag{20}$$

When $n \to \infty$, obviously, there is

$$\begin{aligned}
\sum_{k=0}^{n}\mathbb{E}\{\|\xi_\varkappa(k)\|^2\} \leq&\frac{1}{\hbar}(\mathbb{E}\{V_\varkappa(n+1, \varsigma, \varrho)\} - \mathbb{E}\{V_\varkappa(0, \varsigma, \varrho)\}) \\
\leq&\frac{1}{\hbar}V_\varkappa(0, \varsigma, \varrho)\} < \infty.
\end{aligned} \tag{21}$$

This indicates that all agents maintain stochastic consensus, with the proof being completed. □

Theorem 2. *If there exists a matrix $P_{\varsigma\varrho} > 0$ ($\varsigma \in \mathcal{M}, \varrho \in \mathcal{N}$) that ensures the DTMJFOMASs (14) is stochastic consensus stability with the H_∞ performance level μ, then for any scalar $0 \leq \varkappa \leq n-1$, the following condition holds:*

$$\Sigma_{\varkappa}^{\varsigma\varrho} = \begin{bmatrix} \Sigma_{11} & 0 & 0 & \Lambda_{13} \\ * & -\mu^2 I & 0 & \mathcal{D}_\varsigma \\ * & * & -I & \Lambda_{23} \\ * & * & * & -\mathcal{P}_{\varsigma\varrho}^{-1} \end{bmatrix} < 0, \tag{22}$$

where $\Sigma_{11} = \mathcal{E}_\varsigma^T \mathcal{E}_\varsigma + \Lambda_{11}$.

Proof. To consider the H_∞ performance of the system (14), we define

$$\begin{aligned} \mathcal{J}(k) =& \mathbb{E}\{\triangle V_\varkappa(k,\varsigma,\varrho) + \hat{z}_\varkappa^T(k)\hat{z}_\varkappa(k) - \mu^2\hat{\omega}_\varkappa^T(k)\hat{\omega}_\varkappa(k)\} \\ =& \hat{x}_\varkappa^T(k)[\mathcal{A}_\varsigma + \gamma_\varkappa \mathcal{B}_\varsigma K_\varsigma(I+\mathcal{H}_\varrho)\mathcal{C}_\varsigma]^T \mathcal{P}_{\varsigma\varrho}[\mathcal{A}_\varsigma + \gamma_\varkappa \mathcal{B}_\varsigma K_\varsigma(I+\mathcal{H}_\varrho)\mathcal{C}_\varsigma]\hat{x}_\varkappa(k) \\ &+ \hat{e}_\varkappa^T(k)[\gamma_\varkappa \mathcal{B}_\varsigma K_\varsigma(I+\mathcal{H}_\varrho)]^T \mathcal{P}_{\varsigma\varrho}[\gamma_\varkappa \mathcal{B}_\varsigma K_\varsigma(I+\mathcal{H}_\varrho)]\hat{e}_\varkappa(k) + \hat{\omega}_\varkappa^T(k)\mathcal{D}_\varsigma^T \mathcal{P}_{\varsigma\varrho}\mathcal{D}_\varsigma\hat{\omega}_\varkappa(k) \\ &+ \hat{x}_\varkappa^T(k)\mathcal{E}_\varsigma^T\mathcal{E}_\varsigma\hat{x}_\varkappa(k) + \hat{x}_\varkappa^T(k)\mathcal{C}_\varsigma^T\mathcal{C}_\varsigma\hat{x}_\varkappa(k) - \hat{e}_\varkappa^T(k)\hat{e}_\varkappa(k) - \hat{x}_\varkappa^T(k)P_{\varsigma\varrho}\hat{x}_\varkappa(k) - \mu^2\hat{\omega}_\varkappa^T(k)\hat{\omega}_\varkappa(k) \\ =& \hat{\xi}_\varkappa^T(k)\Sigma_\varkappa^{\varsigma\varrho}\hat{\xi}_\varkappa(k), \end{aligned} \tag{23}$$

where $\hat{\xi}_\varkappa^T(k) = [\hat{x}_\varkappa^T(k),\ \hat{e}_\varkappa^T(k),\ \hat{\omega}_\varkappa^T(k)]^T$.

According to (22), one obtains $\mathcal{J}(k) < 0$. Likewise, we can conclude that

$$\sum_{k=0}^{\infty} \mathbb{E}\{\hat{z}_\varkappa^T(k)\hat{z}_\varkappa(k)\} < \mathbb{E}\{V_\varkappa(\infty,\varsigma,\varrho)\} - \mathbb{E}\{V_\varkappa(0,\varsigma,\varrho)\} + \mu^2 \sum_{k=0}^{\infty} \mathbb{E}\{\hat{\omega}_\varkappa^T(k)\hat{\omega}_\varkappa(k)\}. \tag{24}$$

According to (24), $\mathbb{E}\{\hat{z}_\varkappa^T(k)\hat{z}_\varkappa(k) - \mu^2\hat{\omega}_\varkappa^T(k)\hat{\omega}_\varkappa(k)\} < 0$. This indicates that the DTMJ-FOMASs (14) maintain stochastic H_∞ consistent stability. This completes the proof. □

Theorem 3. *If there exist matrices $P_{\varsigma\varrho} > 0$ ($\varsigma \in \mathcal{M}, \varrho \in \mathcal{N}$) and $\mathcal{Z}_\varsigma$ that ensure that the DTMJFOMASs (14) have stochastic consensus stability with the H_∞ performance level μ, then for any scalars $\varkappa$, ε, ε_1, and ε_2, the following condition holds:*

$$\Xi_{\varkappa}^{\varsigma\varrho} = \begin{bmatrix} \Xi_{11} & 0 & 0 & \Xi_{14} & \Xi_{15} & 0 \\ * & -\mu^2 I & 0 & \Xi_{24} & 0 & 0 \\ * & * & -I & \Xi_{34} & 0 & 0 \\ * & * & * & \Xi_{44} & 0 & \Xi_{46} \\ * & * & * & * & \Xi_{55} & \Xi_{56} \\ * & * & * & * & * & \Xi_{66} \end{bmatrix} < 0, \tag{25}$$

where
$\Xi_{11} = \mathcal{E}_\varsigma^T\mathcal{E}_\varsigma - P_{\varsigma\varrho} - (\varepsilon_1+\varepsilon_2)\mathcal{C}_\varsigma^T\mathcal{C}_\varsigma$,
$\Xi_{14} = (\mathcal{Z}_\varsigma\mathcal{A}_\varsigma + \gamma_\varkappa\mathcal{B}_\varsigma\mathcal{Y}_\varsigma\mathcal{C}_\varsigma)^T$,
$\Xi_{15} = \varepsilon(\mathcal{Y}_\varsigma\mathcal{C}_\varsigma)^T - \gamma_\varkappa(\mathcal{Z}_\varsigma\mathcal{B}_\varsigma - \mathcal{B}_\varsigma\mathcal{X}_\varrho)$,
$\Xi_{24} = (\mathcal{Z}_\varsigma\mathcal{D}_\varsigma)^T$,
$\Xi_{34} = (\gamma_\varkappa\mathcal{Z}_\varsigma\mathcal{B}_\varsigma\mathcal{Y}_\varsigma)^T - \mathcal{Z}_\varsigma^T$,
$\Xi_{44} = \mathcal{P}_{\varsigma\varrho}^{-1} - \mathcal{Z}_\varsigma - \mathcal{Z}_\varsigma^T$,
$\Xi_{46} = [-\gamma_\varkappa\mathcal{B}_\varsigma\mathcal{Y}_\varsigma\ 0]$,
$\Xi_{55} = -\varepsilon(\mathcal{X}_\varsigma + \mathcal{X}_\varsigma^T)$,
$\Xi_{56} = [0\ \varepsilon\mathcal{Y}_\varsigma]$,
$\Xi_{66} = \mathrm{diag}\{-\varepsilon_1 I,\ \varepsilon_2 I\}$.

The controller gain matrix can be obtained according to the following equation:

$$K_\varsigma = Y_\varsigma^T \mathcal{Z}_\varsigma^{-T}. \tag{26}$$

Proof. Given the inequality $(\mathcal{P}_{\varsigma\varrho} - \mathcal{Z}_\varsigma)\mathcal{P}_{\varsigma\varrho}^{-1}(\mathcal{P}_{\varsigma\varrho} - \mathcal{Z}_\varsigma)^T \geq 0$, one can deduce that

$$-\mathcal{Z}_\varsigma \mathcal{P}_{\varsigma\varrho}^{-1}\mathcal{Z}_\varsigma^T \leq \mathcal{P}_{\varsigma\varrho} - \mathcal{Z}_\varsigma - \mathcal{Z}_\varsigma^T, \tag{27}$$

Leveraging Lemmas 1 and 2, one can derive from Equation (25) that

$$\begin{bmatrix} \widetilde{\Xi}_{11} & 0 & 0 & \widetilde{\Xi}_{14} & \widetilde{\Xi}_{15} \\ * & -\mu^2 I & 0 & \Xi_{24} & 0 \\ * & * & -I & \Xi_{34} & 0 \\ * & * & * & \widetilde{\Xi}_{44} & 0 \\ * & * & * & * & \Xi_{55} \end{bmatrix} < 0, \tag{28}$$

where
$\widetilde{\Xi}_{11} = \mathcal{E}_\varsigma^T \mathcal{E}_\varsigma - P_{\varsigma\varrho}$,
$\widetilde{\Xi}_{14} = \Xi_{14} - (\gamma_\varkappa \mathcal{B}_\varsigma \mathcal{Y}_\varsigma \mathcal{C}_\varsigma)^T$,
$\widetilde{\Xi}_{15} = \varepsilon(\mathcal{Y}_\varsigma(I + \mathcal{H}_\varrho)\mathcal{C}_\varsigma)^T - \gamma_\varkappa(\mathcal{Z}_\varsigma \mathcal{B}_\varsigma - \mathcal{B}_\varsigma \mathcal{X}_\varrho)$,
$\widetilde{\Xi}_{44} = -\mathcal{Z}_\varsigma \mathcal{P}_{\varsigma\varrho}^{-1}\mathcal{Z}_\varsigma^T$.

Through the application of Lemma 3, it is possible to infer from (28) that

$$\Xi_\varkappa^{\varsigma\varrho} = \begin{bmatrix} \widetilde{\Xi}_{11} & 0 & 0 & \overline{\Xi}_{14} \\ * & -\mu^2 I & 0 & \Xi_{23} \\ * & * & -I & \Xi_{34} \\ * & * & * & \widetilde{\Xi}_{44} \end{bmatrix} < 0, \tag{29}$$

where
$\overline{\Xi}_{14} = \widetilde{\Xi}_{14} - \gamma_\varkappa((\mathcal{Z}_\varsigma \mathcal{B}_\varsigma - \mathcal{B}_\varsigma \mathcal{X}_\varrho)\mathcal{X}_\varsigma^{-1}\mathcal{Y}_\varsigma(I + \mathcal{H}_\varrho)\mathcal{C}_\varsigma)^T$.

Following this, pre-multiplying and post-multiplying (29) with $\mathrm{diag}\{I,\ I,\ I,\ \mathcal{Z}_\varsigma^{-1}\}$ and its transpose lead to the straightforward observation that Equation (22) holds. This indicates that the system (14) achieves consensus at the H_∞ performance level μ. The proof is finalized. □

5. Simulation Examples

In this section, the feasibility and practicality of the proposed method are illustrated through a numerical example and a single-link robotic arm demonstration.

5.1. A Numerical Example

Consider the DTMJFOMASs composed of four agents, as depicted in Figure 2. The corresponding Laplacian matrix L is as follows:

$$L = \begin{bmatrix} 1 & -1 & 0 & 0 \\ 0 & 1 & -1 & 0 \\ -1 & 0 & 2 & 0 \\ 0 & -1 & 0 & 1 \end{bmatrix}.$$

The TPMs Π and Θ with incomplete transition probabilities in Markov jump modes are as follows:

$$\Pi = \begin{bmatrix} 0.3 & 0.1 & 0.6 \\ 0.6 & * & * \\ 0.2 & * & * \end{bmatrix},\ \Theta = \begin{bmatrix} 0.2 & 0.6 & 0.2 \\ 0.5 & * & * \\ * & * & 0.8 \end{bmatrix}.$$

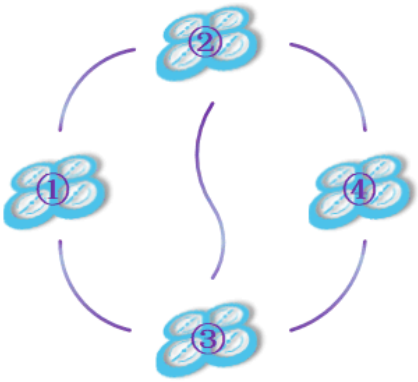

Figure 2. The topological structure of four agents.

The matrix parameters are shown in Table 1. The initial state of four agents are set as $x_1(0) = [1,\ -1]^T$, $x_2(0) = [-5,\ 8]^T$, $x_3(0) = [3,\ -2]^T$, $x_4(0) = [2,\ 5]^T$, and $c = 1$. The disturbance input is designated as $\omega(k) = 0.05e^{-0.05k}\sin(k)$. The stochastic packet loss probability is given by $\bar{\beta} = 20\%$. The initial values of QETM are established as $\delta_\varrho = 0.55$, $v_{\min} = 0.01$, $\varrho_1 = 0.1$, $\varrho_2 = 0.99$, and $\varepsilon_0 = 0.45$.

Table 1. The matrix parameters for three modes.

	A	B	C	D	E
Mode 1	$\begin{bmatrix} 0.95 & 0.01 \\ 0.15 & 0.95 \end{bmatrix}$	$\begin{bmatrix} 0.51 & -0.1 \\ 0.05 & 0.15 \end{bmatrix}$	$\begin{bmatrix} 0.2 & 0.1 \end{bmatrix}$	$\begin{bmatrix} 0.02 \\ 0.1 \end{bmatrix}$	$\begin{bmatrix} 0.1 & 0.1 \end{bmatrix}$
Mode 2	$\begin{bmatrix} 0.96 & 0.02 \\ 0.15 & 0.8 \end{bmatrix}$	$\begin{bmatrix} 0.01 & -0.1 \\ 0.05 & 0.1 \end{bmatrix}$	$\begin{bmatrix} 0.21 & 0.08 \end{bmatrix}$	$\begin{bmatrix} 0.01 \\ 0.1 \end{bmatrix}$	$\begin{bmatrix} 0.14 & -0.1 \end{bmatrix}$
Mode 3	$\begin{bmatrix} 0.95 & 0.02 \\ 0.1 & 0.98 \end{bmatrix}$	$\begin{bmatrix} 0.49 & -0.1 \\ 0.05 & 0.01 \end{bmatrix}$	$\begin{bmatrix} 0.2 & 0.11 \end{bmatrix}$	$\begin{bmatrix} 0.05 \\ 0.1 \end{bmatrix}$	$\begin{bmatrix} -0.1 & 0.14 \end{bmatrix}$

By solving LMIs in Theorem 3, we obtain that optimal H_∞ performance index $\mu = 1.2595$ and controller gains

$$K_1 = [1.5250,\ 1.1883]^T,\ K_2 = [1.5195,\ 0.5143]^T,\ K_3 = [0.4502,\ 0.1514]^T.$$

The state trajectory diagrams for four agents are depicted without control input and with control input in Figure 3a,b, respectively. Obviously, the agents without control input fail to converge, whereas the agents under the influence of the distributed controller (9) can realize consensus. This indicates that the distributed control algorithm introduced in the study is genuinely effective.

As depicted in Figure 4, the control output is displayed under the scenario of DoS attacks. Notably, system (14) maintains strong robustness even when confronted with DoS attacks. The evolution of modes ψ and ϕ are presented in Figure 5. By examining the error curve in Figure 6, it is clear that the agents achieve consensus by 43 s. Figure 7 demonstrates the triggering time interval for all agents. The average triggering frequency of multiagents is 7.25%. The comparison between the measurement output $y(k)$ and the quantized output $\eta(k)$ is illustrated in Figure 8. The results indicate that the QETM proposed not only saves communication channels but also ensures consensus among multiagents.

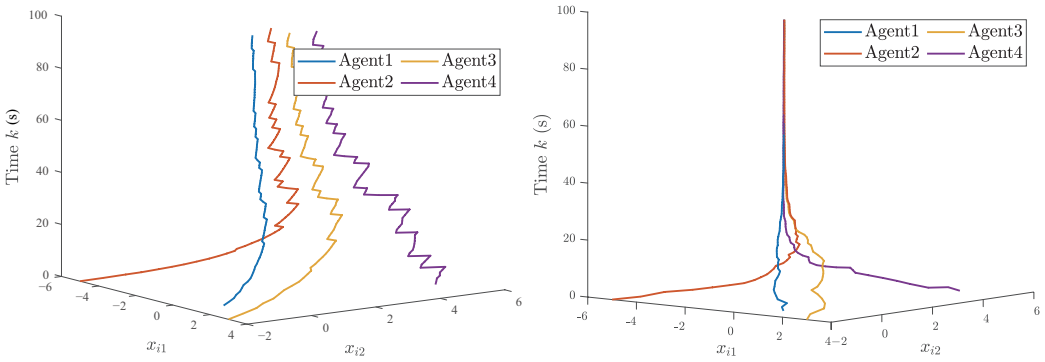

(**a**) (**b**)

Figure 3. The 3D state trajectory of four agents. (**a**) Without control input. (**b**) With control input.

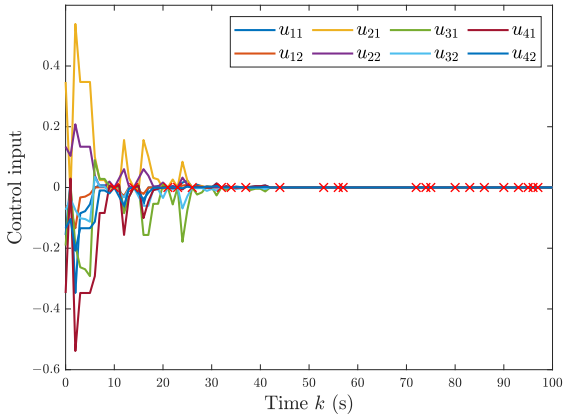

Figure 4. The control input of four agents with DoS attacks.

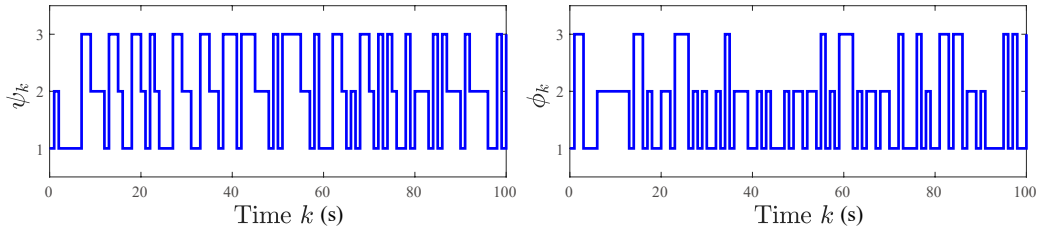

(**a**) (**b**)

Figure 5. The evolution of modes ψ and ϕ. (**a**) Mode ψ. (**b**) Mode ϕ.

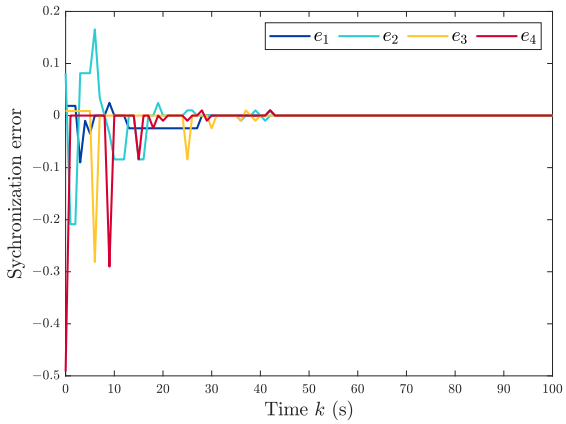

Figure 6. The error curve of four agents.

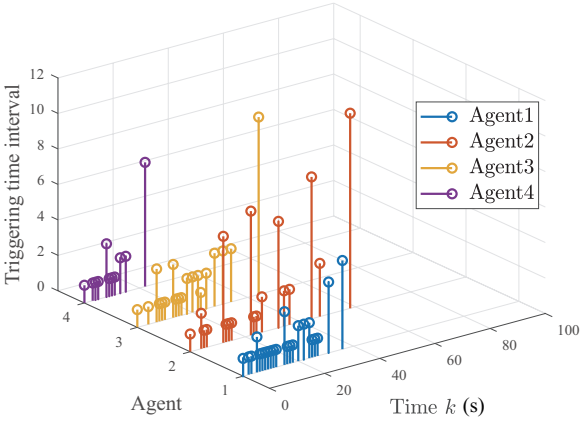

Figure 7. The triggering time interval of four agents. The trigger frequencies for agent 1–4 are 5%,

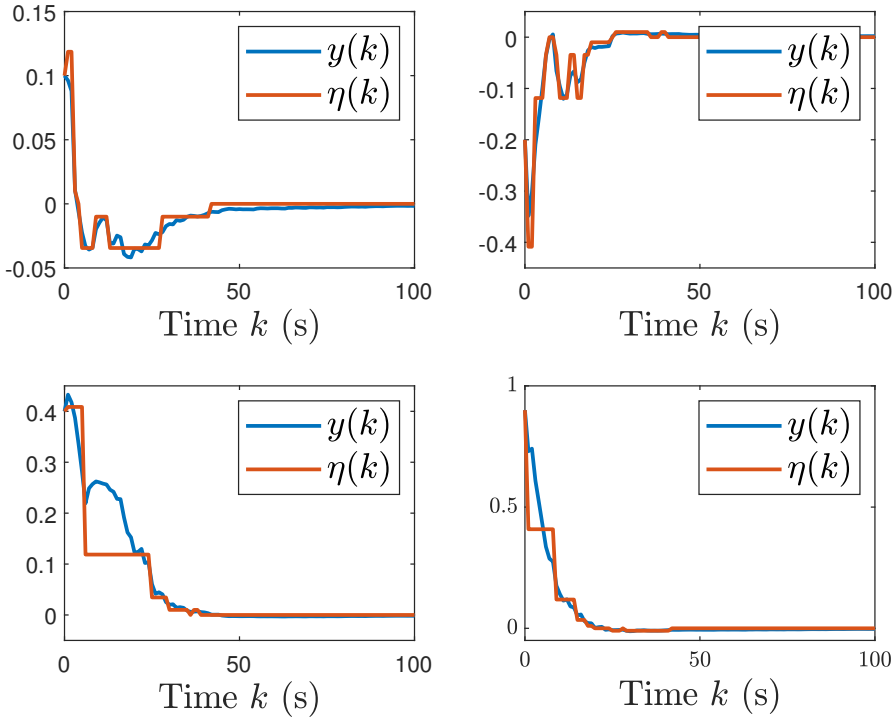

Figure 8. The measurement output $y(k)$ and the quantized output $\eta(k)$ of four agents.

5.2. The Single-Link Robotic Arm Systems

We validate the model's practicability through the SLRASs with six nodes [2,47–50], with its dynamic equation being formulated as

$$J\ddot{\theta}(t) = -glM\sin(\theta(t)) - R\dot{\theta}(t) + u(t)$$

where $\theta(t)$, J, and M stand for the angle position of the arm, the mass of payload, and the moment of inertia, respectively. The gravity acceleration g, the arm length L, and the payload mass M take the value 9.81 m/s^2, 0.5 m, and 2 N $\cdot$ m/s, respectively. The dynamic mode of the SLRASs can be expressed as

$$\begin{cases} x_\varkappa(k+1) = \mathcal{A}_\varsigma x_\varkappa(k) + \mathcal{B}_\varsigma u_\varkappa(k) + \mathcal{D}_\varsigma \omega_\varkappa(k) \\ y_\varkappa(k) = \mathcal{C}_\varsigma x_\varkappa(k) \end{cases}$$

where $A_\varsigma = \begin{bmatrix} 1 & T \\ -\frac{TgLM}{J} & 1-\frac{TR}{J} \end{bmatrix}$, $B_\varsigma = \begin{bmatrix} 0 & T \\ 0 & -\frac{TR}{J} \end{bmatrix}$, $D_\varsigma \begin{bmatrix} 0 \\ T \end{bmatrix}$.

There are three different modes for the parameters J and M: $J_1 = 1\ \mathrm{N}\cdot\mathrm{m},\ M_1 = 1\ \mathrm{kg}$; $J_2 = 2.5\ \mathrm{N}\cdot\mathrm{m},\ M_2 = 2\ \mathrm{kg}$; $J_3 = 5\ \mathrm{N}\cdot\mathrm{m},\ M_3 = 4\ \mathrm{kg}$. The sampling period is $T = 0.1$ s, $f = 0.01/\pi$. The TPMs Π and Θ are as follows:

$$\Pi = \begin{bmatrix} 0.3 & 0.2 & 0.5 \\ * & * & 0.5 \\ 0.4 & * & * \end{bmatrix},\ \Theta = \begin{bmatrix} 0.1 & * & * \\ 0.4 & * & * \\ * & 0.2 & * \end{bmatrix}.$$

The directed topology structure of the SLRASs is depicted in Figure 9. The corresponding Laplacian matrix is as follows:

$$L = \begin{bmatrix} 1 & -1 & 0 & 0 & 0 & 0 \\ -1 & 2 & -1 & 0 & 0 & 0 \\ 0 & -1 & 2 & -1 & 0 & 0 \\ 0 & -1 & -1 & 3 & -1 & 0 \\ 0 & 0 & 0 & -1 & 2 & -1 \\ 0 & 0 & -1 & 0 & 0 & 1 \end{bmatrix}.$$

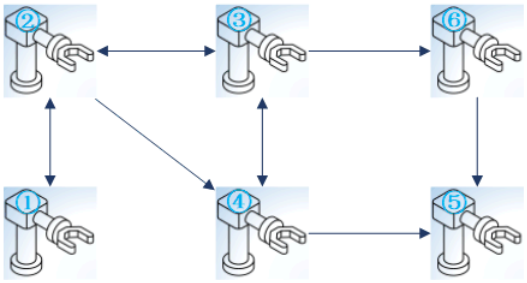

Figure 9. The directed topology structure of the SLRASs.

The matrix parameters are defined in Table 2. The initial state of the SLRASs are configured as $x_1(0) = [10,\ -10]^T$, $x_2(0) = [-5,\ 8]^T$, $x_3(0) = [33,\ -28]^T$, $x_4(0) = [14,\ 35]^T$, $x_5(0) = [-35,\ 22]^T$, $x_6(0) = [21,\ 16]^T$, and $c = 10.05$. We set the disturbance input as $\omega(k) = e^{-0.05k}\sin(0.1\pi k)$.

Table 2. The matrix parameters of the SLRASs.

	A	B	C	D	E
Mode 1	$\begin{bmatrix} 1 & 0.1 \\ -4.9505 & -1 \end{bmatrix}$	$\begin{bmatrix} 0 & 0.1 \\ 0 & -0.2 \end{bmatrix}$	$\begin{bmatrix} 0 & 0.1 \end{bmatrix}$	$\begin{bmatrix} 0 \\ 0.1 \end{bmatrix}$	$\begin{bmatrix} 0.1 & 0.1 \end{bmatrix}$
Mode 2	$\begin{bmatrix} 1 & 0.1 \\ -3.9240 & 0.2 \end{bmatrix}$	$\begin{bmatrix} 0 & 0.1 \\ 0 & -0.8 \end{bmatrix}$	$\begin{bmatrix} 0 & 0.04 \end{bmatrix}$	$\begin{bmatrix} 0 \\ 0.1 \end{bmatrix}$	$\begin{bmatrix} 0.14 & -0.1 \end{bmatrix}$
Mode 3	$\begin{bmatrix} 1 & 0.1 \\ -2.4525 & 0.8 \end{bmatrix}$	$\begin{bmatrix} 0 & 0.1 \\ 0 & -0.02 \end{bmatrix}$	$\begin{bmatrix} 0 & 0.01 \end{bmatrix}$	$\begin{bmatrix} 0 \\ 0.1 \end{bmatrix}$	$\begin{bmatrix} -0.1 & 0.14 \end{bmatrix}$

Utilizing Theorem 3, we ascertain optimal H_∞ performance index $\mu = 1.9523$ and controller gains

$$K_1 = [0.0525,\ 0.0218]^T,\ K_2 = [-0.5200,\ -0.4143]^T,\ K_3 = [0.0515,\ 0.0555]^T.$$

Figure 10 shows the mode ψ and ϕ evolution in the SLRASs. Figures 11–14 illustrate the SLRASs consensus simulation under DoS attacks, and it is evident that the state converges to zero after 22 s. In Figures 11 and 12, the control input and output for the SLRASs are presented. The error curve for the SLRASs is displayed in Figure 13. The 3D

state trajectory for the SLRASs is depicted in Figure 14. Table 3 illustrates the triggering frequencies and their averages for each robotic arm under QETM, Method 1, and Method 2. Method 1 and Method 2 construct new triggering mechanisms by integrating the logarithmic quantizer in [35] and the uniform quantizer in [31,32] with Equation (8). Overall, the controller presented in this paper maintains consensus under DoS attack and minimizes communication loads efficiently.

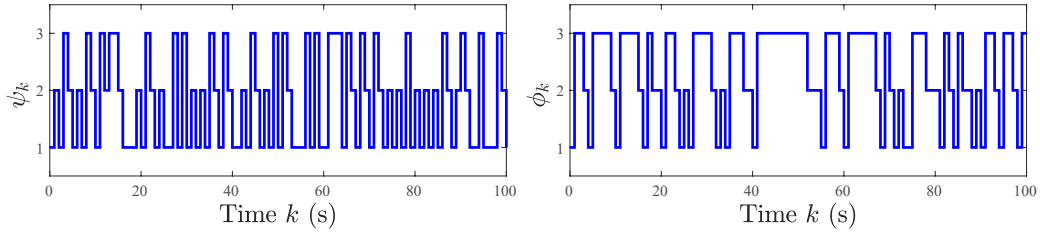

(**a**) (**b**)

Figure 10. The evolution of modes ψ and ϕ. (**a**) Mode ψ. (**b**) Mode ϕ.

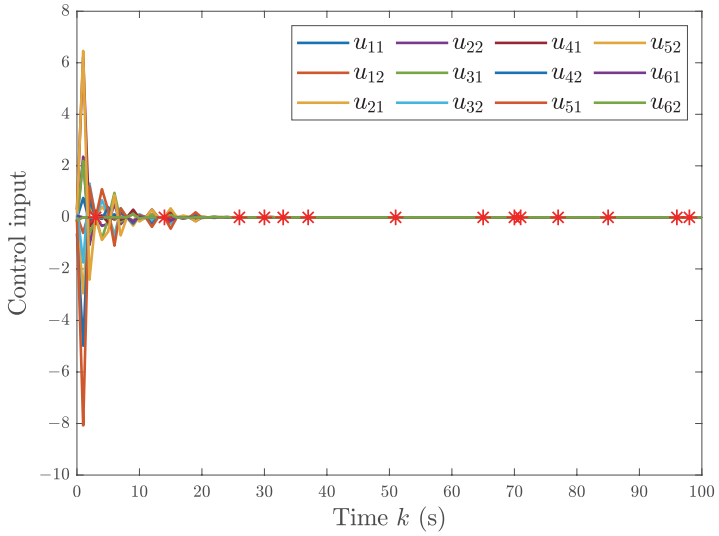

Figure 11. The control input of the SLRASs with DoS attacks.

Table 3. The trigger frequency of all robotic arms.

Trigger Frequency	Robotic Arm 1	Robotic Arm 2	Robotic Arm 3	Robotic Arm 4	Robotic Arm 5	Robotic Arm 6	Average
QETM	18%	23%	21%	19%	24%	23%	21.33%
Method 1 *	23%	24%	24%	26%	21%	26%	24.00%
Method 2 *	38%	35%	40%	33%	30%	33%	34.83%

* Method 1 and Method 2 construct new triggering mechanisms by integrating the logarithmic quantizer in [35] and the uniform quantizer in [31,32] with Equation (8).

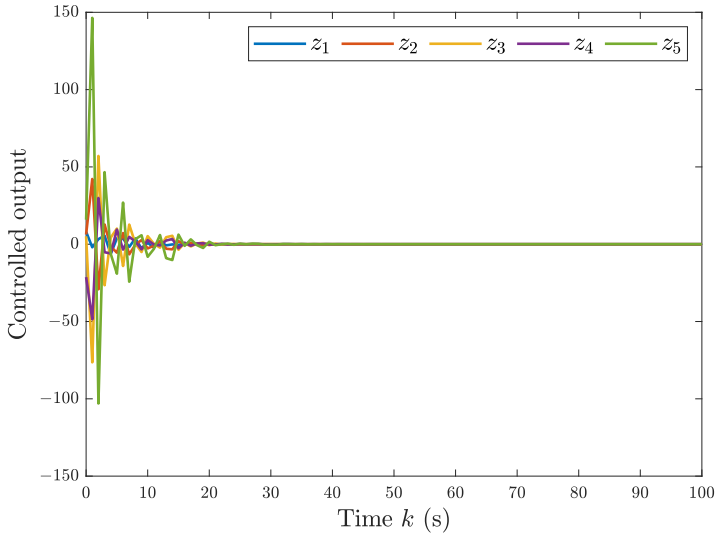

Figure 12. The controlled output of the SLRASs.

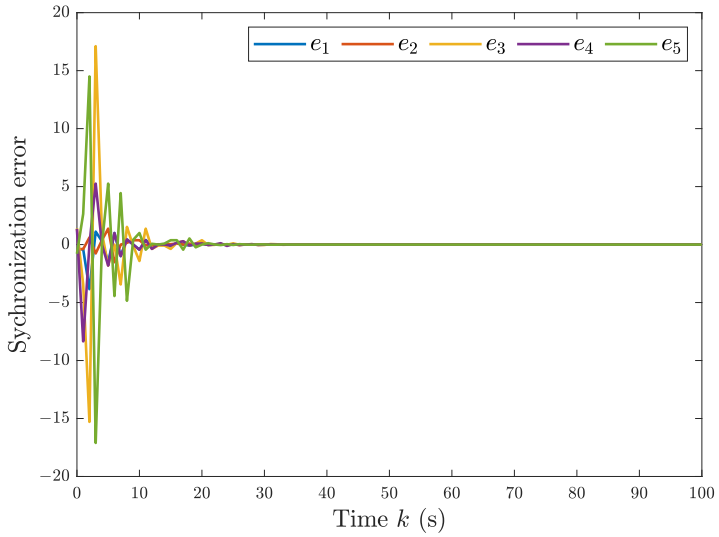

Figure 13. The error curve of the SLRASs.

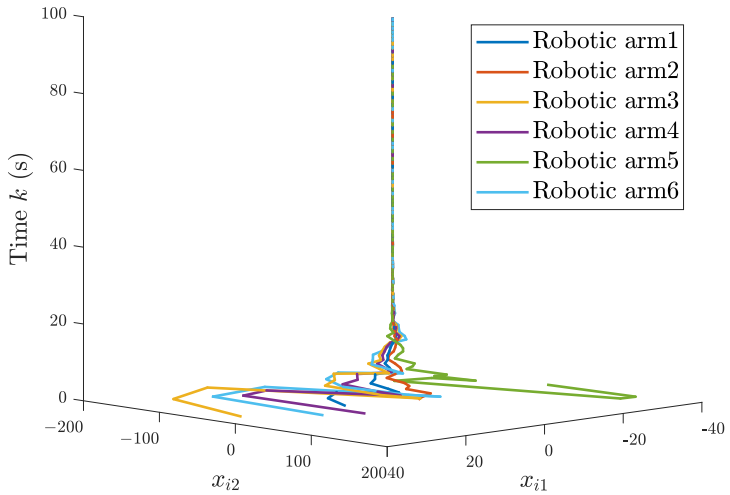

Figure 14. The 3D state trajectory of the SLRASs with controller.

6. Conclusions

This paper examines the H_∞ consensus control of DTMJFOMASs with DoS attacks and external disturbances, extending the short-memory principle proposed in reference [23] to MJMASs. To conserve bandwidth and minimize triggering frequency, the mode-dependent QETM is employed. According to the designed distributed controller, sufficient conditions are proposed to ensure the system consensus under the given H_∞ performance criterion. In the end, the validity and applicability of the proposed model are elucidated through a numeric example and the SLRASs.

It is worth noting that this paper only considers linear time-invariant DTMJFOMASs. Future research will concentrate on addressing the problem of leader–follower consensus in nonlinear DTMJFOMASs. Additionally, our objectives include designing a triggering mechanism that can more effectively conserve communication resources, thereby further optimizing system performance.

Author Contributions: Writing—original draft preparation: Y.L.; writing—review and editing: Y.L. and X.W.; methodology: Y.L.; software: Y.L.; supervision: X.W., Y.W. and L.H.; investigation: X.W., Y.W. and L.H.; formal analysis: Y.L., X.W., Y.W. and Q.W.; and funding acquisition, X.W. and Q.W. All authors have read and agreed to the published version of the manuscript.

Funding: This work was supported by National Natural Science Foundation of China under Grant 62263005, Guangxi Natural Science Foundation under Grant 2020GXNSFDA238029, and Key Laboratory of AI and Information Processing (Hechi University), Education Department of Guangxi Zhuang Autonomous Region under Grant 2022GXZDSY004.

Data Availability Statement: Data are contained within the article.

Conflicts of Interest: The authors declare no conflict of interest.

References

1. Ren, W.; Sorensen, N. Distributed coordination architecture for multi-robot formation control. *Rob. Auton. Syst.* **2008**, *56*, 324–333. [CrossRef]
2. Yang, X.; Yuan, J.; Chen, T.; Zhang, C.; Yang, H.; Hu, S. Distributed convex optimization of higher order nonlinear uncertain multi-agent systems with switched parameters and topologies. *J. Vib. Control* **2023**. [CrossRef]
3. Pipattanasomporn, M.; Feroze, H.; Rahman, S. Multi-agent systems in a distributed smart grid: Design and implementation. In Proceedings of the 2009 IEEE/PES Power Systems Conference and Exposition, Seattle, WA, USA, 15–18 March 2009; pp. 1–8. [CrossRef]
4. Pang, K.; Ma, L.; Bai, H.; Yi, X. Dynamic event-based finite-horizon H_∞ secure consensus control of a class of nonlinear multi-agent systems. *ISA Trans.* **2022**, *127*, 168–177. [CrossRef]
5. Ding, P.; Shen, H.; Xia, J.; Li, F. H_∞ secure consensus of hidden Markov jump multi-agent systems subject to DoS attacks and disturbance. *Int. J. Robust Nonlinear Control* **2024**. [CrossRef]
6. Xue, A.; Wang, H.; Lu, R. Event-based $H\infty$ control for discrete Markov jump systems. *Neurocomputing* **2016**, *190*, 165–171. [CrossRef]
7. Yao, L.; Huang, X.; Wang, Z.; Liu, K. Secure control of Markovian jumping systems under deception attacks: An attack-probability-dependent adaptive event-trigger mechanism. *IEEE Trans. Control Netw. Syst.* **2023**, *10*, 1818–1830. [CrossRef]
8. Li, S.; Chen, Y.; Liu, P.X. Fault estimation and fault-tolerant tracking control for multi-agent systems with Lipschitz nonlinearities using double periodic event-triggered mechanism. *IEEE Trans. Signal Inf. Process. Netw.* **2023**, *9*, 229–241. [CrossRef]
9. Guo, S.; Zhao, X.; Wang, H.; Xu, N. Distributed consensus of heterogeneous switched nonlinear multiagent systems with input quantization and DoS attacks. *Appl. Math. Comput.* **2023**, *456*, 128127. [CrossRef]
10. Wang, X.; Niu, B.; Gao, Y.; Shang, Z. Adaptive finite time output feedback bipartite tracking control for nonlinear multiagent systems. *IEEE Trans. Autom. Sci. Eng.* **2023**. [CrossRef]
11. Chai, J.; Lu, Q.; Tao, X.; Peng, D.; Zhang, B. Dynamic event-triggered fixed-time consensus control and its applications to magnetic map construction. *IEEE/CAA J. Autom. Sin.* **2023**, *10*, 2000–2013. [CrossRef]
12. Costa, O.L.V.; Fragoso, M.D.; Marques, R.P. Discrete-time Markov jump linear systems. Springer Science & Business Media, 2005.
13. Lian, J.; Li, S. Fuzzy control of uncertain positive Markov jump fuzzy systems with input constraint. *IEEE Trans. Cybern.* **2021**, *51*, 2032–2041. [CrossRef]
14. Sakthivel, R.; Parivallal, A.; Kaviarasan, B.; Lee, H.; Lim, Y. Finite-time consensus of Markov jumping multi-agent systems with time-varying actuator faults and input saturation. *ISA Trans.* **2018**, *83*, 89–99. [CrossRef]
15. Yang, H.; Zhang, H.; Wang, Z.; Yan, H. Reliable leader-following consensus of discrete-time semi-Markovian jump multi-agent systems. *IEEE Trans. Netw. Sci. Eng.* **2023**, *10*, 3505–3518. [CrossRef]

16. Dong, S.; Ren, W.; Wu, Z.G.; Su, H. H_∞ output consensus for Markov jump multiagent systems with uncertainties. *IEEE Trans. Cybern.* **2022**, *50*, 2264–2273. [CrossRef]
17. Wang, H.; Xue, B.; Xue, A. Leader-following consensus control for semi-Markov jump multi-agent systems: An adaptive event-triggered scheme. *J. Franklin Inst.* **2021**, *358*, 428–447. [CrossRef]
18. Huo, S.; Zhang, Y. $H\infty$ consensus of Markovian jump multi-agent systems under multi-channel transmission via output feedback control strategy. *ISA Trans.* **2020**, *99*, 28–36. [CrossRef]
19. Dong, S.; Liu, L.; Feng, G.; Liu, M.; Wu, Z.G.; Zheng, R. Cooperative output regulation quadratic control for discrete-time heterogeneous multiagent Markov jump systems. *IEEE Trans. Cybern.* **2022**, *52*, 9882–9892. [CrossRef]
20. Wang, J.; Chen, X. $H\infty$ consensus for stochastic Markov jump multi-agent systems with imperfect time-varying transition probabilities and multiplicative noise. *Appl. Math. Comput.* **2023**, *436*, 127504. [CrossRef]
21. Abdelwahed, H.; El-Shewy, E.; Alghanim, S.; Abdelrahman, M.A. On the physical fractional modulations on Langmuir plasma structures. *Fractal Fract.* **2022**, *6*, 430. [CrossRef]
22. Sharaf, M.; El-Shewy, E.; Zahran, M. Fractional anisotropic diffusion equation in cylindrical brush model. *J. Taibah Univ. Sci.* **2020**, *14*, 1416–1420. [CrossRef]
23. An, C.; Su, H.; Chen, S. H_∞ consensus for discrete-time fractional-order multi-agent systems with disturbance via Q-learning in zero-sum games. *IEEE Trans. Netw. Sci. Eng.* **2022**, *9*, 2803–2814. [CrossRef]
24. Shahamatkhah, E.; Tabatabaei, M. Containment control of linear discrete-time fractional-order multi-agent systems with time-delays. *Neurocomputing* **2020**, *385*, 42–47. [CrossRef]
25. Reed, E.; Chatterjee, S.; Ramos, G.; Bogdan, P.; Pequito, S. Fractional cyber-neural systems-A brief survey. *Annu. Rev. Control* **2022**, *54*, 386–408. [CrossRef]
26. Xu, J.; Cheng, J.; Yan, H.; Park, J.H.;Qi, W. Dynamic event-triggered control for semi-Markov singularly perturbed systems with generally transition rates. *IEEE Trans. Syst. Man Cybern. Syst.* **2024**, *54*, 225–235. [CrossRef]
27. Shi, T.; Shi, P.; Chambers, J. Dynamic event-triggered model predictive control under channel fading and denial-of-service attacks. *IEEE Trans. Autom. Sci. Eng.* **2023**, *54*, 225–235. [CrossRef]
28. Gao, X.; Deng, F.; Zhang, H.; Zeng, P. Observer-based event-triggered asynchronous control of networked Markovian jump systems under deception attacks. *Sci. China Inf. Sci.* **2023**, *66*, 159204. [CrossRef]
29. Hu, Z.; Chen, B. Sliding mode control for multi-agent systems under event-triggering hybrid scheduling strategy. *IEEE Trans. Circuits Syst. II Express Briefs* **2023**. [CrossRef]
30. Wu, Z.G.; Xu, Y.; Pan, Y.J.; Shi, P.; Wang, Q. Event-triggered pinning control for consensus of multiagent systems with quantized information. *IEEE Trans. Syst. Man Cybern. Syst.* **2017**, *48*, 1929–1938. [CrossRef]
31. Zhang, Y.; Wu, Z.G.; Shi, P.; Huang, T.; Chakrabarti, P. Quantization-based event-triggered consensus of multiagent systems against aperiodic DoS attacks. *IEEE Trans. Syst. Man Cybern. Syst.* **2023**, *53*, 3774–3783.[CrossRef]
32. Ren, H.; Liu, R.; Cheng, Z.; Ma, H.; Li, H. Data-driven event-triggered control for nonlinear multi-agent systems with uniform quantization. *IEEE Trans. Circuits Syst. II Express Briefs* **2023**, *71*, 712–716. [CrossRef]
33. Yang, X.; Yuan, J.; Chen, T.; Yang, H. Distributed adaptive optimization algorithm for fractional high-order multiagent systems based on event-triggered strategy and input quantization. *Fractal Fract.* **2023**, *7*, 749. [CrossRef]
34. Wang, Y.; Zhu, F. Distributed dynamic event-triggered control for multi-agent systems with quantization communication. *IEEE Trans. Circuits Syst. II Express Briefs* **2023**. [CrossRef]
35. Arbi, A. Controllability of delayed discret fornasini-marchesini model via quantization and random packet dropouts. *Math. Model. Nat. Phenom.* **2022**, *17*, 38. [CrossRef]
36. Zhou, X.; Tang, Y.; Cheng, J.; Cao, J.; Xue, C.; Yan, D. Nonstationary quantized control for discrete-time Markov jump singularly perturbed systems against deception attacks. *J. Franklin Inst.* **2021**, *358*, 2915–2932. [CrossRef]
37. Zhang, G.; Li, F.; Wang, J.; Shen, H. Mixed $H\infty$ and passive consensus of Markov jump multi-agent systems under DoS attacks with general transition probabilities. *J. Franklin Inst.* **2023**, *360*, 5375–5391. [CrossRef]
38. Li, W.; Niu, Y.; Lv, X. Dynamic event-triggering sliding mode resilient control for multi-agent systems. *J. Franklin Inst.* **2023**, *360*, 10. [CrossRef]
39. Podlubny, I. *Fractional Differential Equations: An Introduction to Fractional Derivatives, Fractional Differential Equations, to Methods of Their Solution and Some of Their Applications*; Elsevier: Amsterdam, The Netherlands, 1998.
40. Zhou, K.; Khargonekar, P.P. Robust stabilization of linear systems with norm-bounded time-varying uncertainty. *Syst. Control Lett.* **1988**, *10*, 17–20. [CrossRef]
41. Ning, Z.; Zhang, L.; de Jesus Rubio, J.; Yin, X. Asynchronous filtering for discrete-time fuzzy affine systems with variable quantization density. *IEEE Trans. Cybern.* **2017**, *47*, 153–164. [CrossRef]
42. Kaczorek, T. *Selected Problems of Fractional Systems Theory*; Springer Science & Business Media: Berlin, Germany, 2011.
43. Wei, Y.; Gao, Y.; Liu, D.Y.; Wang, Y. Controllability and observability of linear nabla fractional order systems. In Proceedings of the 2018 37th Chinese Control Conference, Wuhan, China, 25–27 July 2018; pp. 25–27. [CrossRef]
44. Fu, M.; Xie, L. The sector bound approach to quantized feedback control. *IEEE Trans. Autom. Control* **2005**, *50*, 1698–1711. [CrossRef]
45. Wang, J.; He, W.; Fu, J.; Wang Y.; Sun, J. Sampled-data consensus control of nonlinear multi-agent systems with Markovian switching topologies based on extended looped functional. *IEEE Trans. Circuits Syst. II Express Briefs* **2024**, *71*, 251–255. [CrossRef]

46. Elahi, A.; Alfi, A.; Modares, H. H_∞ consensus control of discrete-time multi-agent systems under network imperfections and external disturbance. *IEEE/CAA J. Autom. Sin.* **2019**, *6*, 667–675. [CrossRef]
47. Zhao, D.; Dong, T.; Hu, W. Event-triggered consensus of discrete time second-order multi-agent network. *Int. J. Control Autom. Syst.* **2018**, *16*, 87–96. [CrossRef]
48. Qi, W.; Zong, G.; Karimi, H.R. Finite-time observer-based sliding mode control for quantized semi-Markov switching systems with application. *IEEE Trans. Ind. Inf.* **2020**, *16*, 1259–1271. [CrossRef]
49. Xue, M.; Yan, H.; Zhang, H.; Li, Z.; Chen, S.; Chen, C. Event-triggered guaranteed cost controller design for T-S fuzzy Markovian jump systems with partly unknown transition probabilities. *IEEE Trans. Fuzzy Syst.* **2021**, *29*, 1052–1064. [CrossRef]
50. Liu, X.; Wei, X.; Li, Y. Observer-based finite-time fuzzy H_∞ control for Markovian jump systems with time-delay and multiplicative noises. *Int. J. Fuzzy Syst.* **2023**, *25*, 1643–1655. [CrossRef]